Table II. Differentially expressed genes in colorectal cancer biopsies and normal colorectal epithelia.

Accession no.	Symbol	Gene definition	Previous report[a]	SNR
Up-regulated genes in cancer biopsies				
NM_181697	**PRDX1**	**peroxiredoxin 1, transcript variant 3**		**2.645**
NM_002128	**HMGB1**	**high-mobility group box 1**	**8,11,15**	**2.364**
NM_003472	**DEK**	**DEK oncogene (DNA binding)**	**11**	**2.341**
NM_001009	RPS5	ribosomal protein S5		2.052
NM_002568	**PABPC1**	**poly(A) binding protein, cytoplasmic 1**	**11,16**	**1.994**
NM_199440	**HSPD1**	**heat shock 60-kDa protein 1 (chaperonin), nuclear gene encoding mitochondrial protein, transcript variant 2**	**10,11,16,19**	**1.985**
NM_021130	**PPIA**	**peptidylprolyl isomerase A (cyclophilin A), transcript variant 1**		**1.957**
BE564899		EST		1.930
NM_001011	RPS7	ribosomal protein S7		1.894
NM_000978	RPL23	ribosomal protein L23		1.878
NM_002954	RPS27A	ribosomal protein S27a		1.860
AK090536		EST		1.826
NM_198829	**RAC1**	**ras-related C3 botulinum toxin substrate 1 (rho family, small GTP binding protein Rac1), transcript variant Rac1c**		**1.814**
NM_000971	RPL7	ribosomal protein L7		1.795
NM_003908	EIF2S2	eukaryotic translation initiation factor 2, subunit 2 ß, 38 kDa		1.772
NM_003756	**EIF3S3**	**eukaryotic translation initiation factor 3, subunit 3 γ, 40 kDa**		**1.763**
NM_000998	RPL37A	ribosomal protein L37a		1.732
NM_021034	**IFITM3**	**interferon induced transmembrane protein 3 (1-8U)**		**1.730**
NM_005381	**NCL**	**nucleolin**	**9**	**1.727**
NM_002106	H2AFZ	H2A histone family, member Z		1.721
Down-regulated genes in cancer biopsies				
NM_174977	SEC14L4	SEC14-like 4 (S. cerevisiae)		-2.518
NM_000067	**CA2**	**carbonic anhydrase II**	**8-11,15,16**	**-2.280**
NM_017958	PLEKHB2	pleckstrin homology domain containing, family B (evectins) member 2		-2.272
NM_005578	**LPP**	**LIM domain containing preferred translocation partner in lipoma**	**18**	**-2.236**
BF826364		EST		-1.926
BC051280		EST		-1.921
NM_003869	**CES2**	**carboxylesterase 2 (intestine, liver), transcript variant 1**	**10,14,16**	**-1.897**
BX647478		EST		-1.834
XM_375330		EST		-1.811
NM_002518	NPAS2	neuronal PAS domain protein 2		-1.789
CD652660		EST		-1.766
NM_020746	KIAA127	KIAA1271 protein		-1.742
NM_000355	TCN2	transcobalamin II; macrocytic anemia		-1.731
NM_005242	F2RL1	coagulation factor II (thrombin) receptor-like 1		-1.728
BM987276		EST		-1.698
XM_370781		**EST**	**16**	**-1.684**
AK129631		FLJ26120		-1.657
NM_002096	GTF2F1	general transcription factor IIF, polypeptide 1, 74 kDa		-1.623
NM_000014	A2M	α-2-macroglobulin		-1.617
NM_020675	Spc25	kinetochore protein Spc25		-1.606

Top 20 up-regulated and 20 down-regulated genes excluding 4 down-regulated genes with no definition, among 692 up-regulated and 219 down-regulated genes in cancer biopsies with SNR ($p<0.001$). Bold: genes reportedly involved in colorectal carcinogenesis based on microarray analysis or genes reportedly involved in carcinogenesis of other cancer types. [a]Previous report on colorectal carcinogenesis using microarray analysis (ref. no.). SNR, signal-to-noise ratio.

Table III. Immunohistochemical staining.

Gene name	Symbol		Expression grade[a]				Staining pattern[b]
			-	1+	2+	3+	
Peroxiredoxin 1	PRDX1	Normal	10				
		Cancer		6	4		Homogeneous
High-mobility group box 1	HMGB1	Normal		10			
		Cancer		1	7	2	Homogeneous
DEK oncogene	DEK	Normal			7	3	
		Cancer		4	6		Heterogeneous
Poly(A) binding protein, cytoplasmic 1	PABPC1	Normal		10			
		Cancer		3	7		Heterogeneous
Heat shock 60-kDa protein 1	HSPD1	Normal	10				
		Cancer			2	8	Homogeneous
Nucleolin	NCL	Normal	4	6			
		Cancer			5	5	Homogeneous
Carbonic anhydrase II	CA2	Normal			4	6	
		Cancer		8	2		Homogeneous

Microarray analyses revealed up-regulation of PRDX1, HMGB1, DEK, PABPC1, HSPD1 and NCL and down-regulation of CA2 in cancers. [a]The mean intensity of immunohistochemical staining in the epithelial or tumor cells evaluated relative to the positive controls as follows: weak, 1+; moderate, 2+; strong, 3+. [b]Intra-tumoral heterogeneity in immunohistochemical staining pattern.

assay. Among the 20 up-regulated genes, 6 genes of ribosomal proteins were included; this finding was in agreement with previous observations (7,9,11,18). In addition, relationships with carcinogenesis of other cancers have been reported regarding PRDX1 (28), peptidylprolyl isomerase A (PPIA) (29), ras-related C3 botulinum toxin substrate 1 (RAC1) (30), eukaryotic translation initiation factor 3, subunit 3 γ (EIF3S3) (31) and interferon induced transmembrane protein 3 (IFITM3) (32).

Immunohistochemical staining. The expression status of encoding proteins from 7 genes in IHC is summarized in Table III. The up- and down-regulation of PRDX1, HMGB1, PABPC1, HSPD1, NCL, and CA2 at the protein level was not in conflict with observations at the transcription level (Table III, Fig. 2). PRDX1, HMGB1, HSPD1, NCL and CA2 showed a homogeneous staining pattern in cancer tissues regardless of the region in the tumors, while the others showed a heterogeneous pattern.

Molecular prediction of tumor malignancy. In the differential diagnosis between 20 cancer biopsies and 20 adenoma biopsies by their gene expression profiles using the supervised classification method, the highest prediction accuracy was 97.5% when 8-71 genes were used (Fig. 3). Comparison between intra- and inter-tumor heterogeneity of the profiles using HCA showed that respective paired biopsies from the same tumors tended to join each other. When the selected 71-gene set with the highest accuracy was used, cancer biopsies and adenoma biopsies were clearly separated, and 18 of 20 paired biopsies were clustered side by side though a small number of genes was used (Fig. 4). Among the 71-gene set, COL1A1, COL1A2, and EIF2S2 were also reported in other studies as useful discriminating genes between cancers and adenomas (11).

Discussion

In the present study, we applied comprehensive expression analysis and found that intra-tumor heterogeneity of the gene expression profiles was smaller than inter-tumor heterogeneity, using preoperative endoscopic biopsies of colorectal tumors. We also showed that tumor malignancy could be accurately diagnosed with the profile in a single biopsy. Such accuracy is a promising first step in the clinical application of this technique for various settings such as prediction of the response to preoperative chemo- and/or radio-therapy or the existence of lymph node metastasis. Our findings suggest that this technique can be potentially used to define accurately the biological properties of colorectal tumors.

In CRC, changes in gene expression profiles that occurred during chemotherapy were detected using rectal cancer biopsies (33). The possible prediction of response to preoperative chemo- and/or radio-therapy for rectal cancers by using gene expression profiling of a single biopsy has also been reported (24,25). However, in the application of diagnosis in the clinical field based on gene expression profiling using preoperative endoscopic biopsies, it is not favorable that the profiles of biopsies from a tumor are widely different from each other. In this regard, our results added support to those

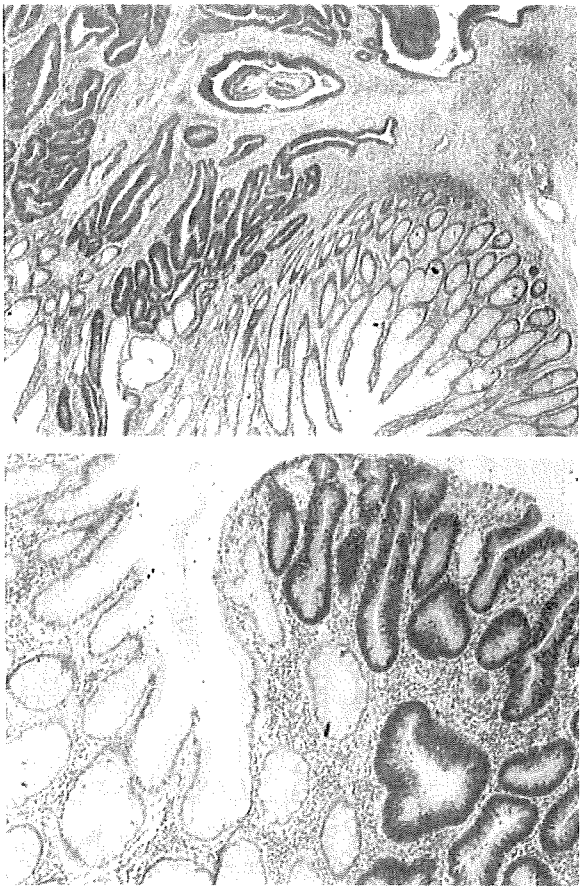

Figure 2. Immunohistochemical staining of HSPD1 (A) and NCL (B) in colorectal cancer tissues. (A) HSPD1 was expressed strongly in cancer cells while no HSPD1 expression was observed in adjacent normal epithelial cells (x4). (B) NCL was expressed strongly in cancer cells and weakly in normal epithelial cells in the lower portion of the colonic gland (x10).

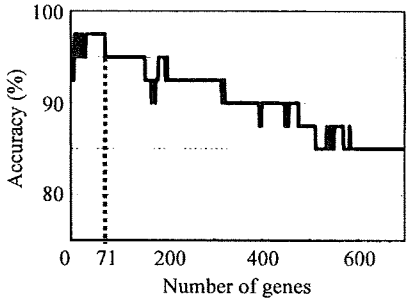

Figure 3. The accuracy curve of the differential diagnosis of 20 cancer biopsies and 20 adenoma biopsies using the supervised classification algorithm. Genes differentially expressed in cancer and adenoma biopsies were ranked according to the signal-to-noise ratio, and the accuracy was calculated with the weighted-votes method and the leave-one-out cross validation. The highest prediction accuracy was 97.5% when 8-71 genes were used.

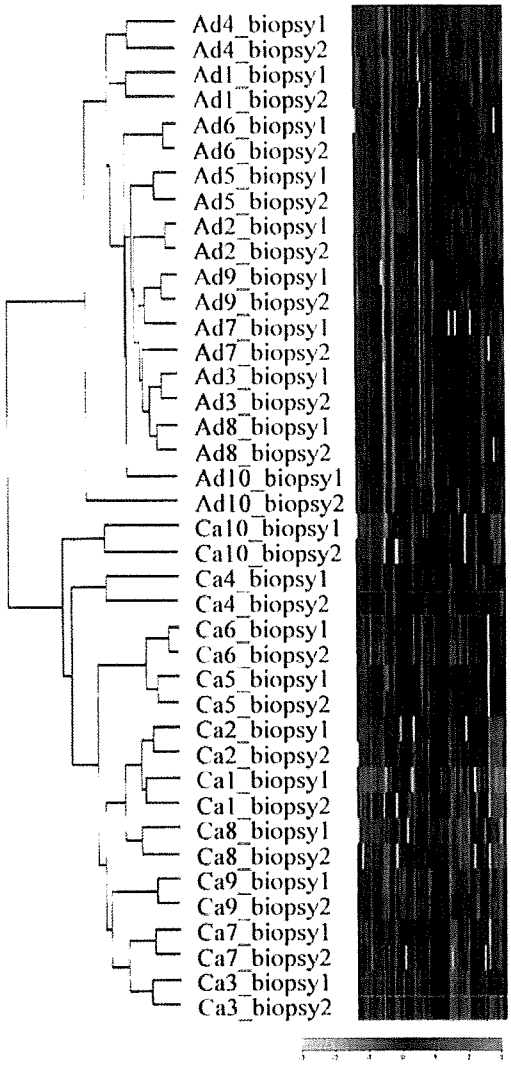

Figure 4. Hierarchical clustering analysis using 71 differentially expressed genes between cancer and adenoma biopsies. Samples consisted of cancer biopsies (n=20; 10 pairs) and adenoma biopsies (n=20; 10 pairs). Pearson's correlation was used as the similarity coefficient and the unweighted pair group method using arithmetic average as the clustering algorithm. Red indicates overexpression, and green indicates underexpression. Cancer biopsies and adenoma biopsies were clearly separated, and 18 of 20 paired biopsies were joined together.

of previous investigators (24,25), thus further promoting the technique.

Through using small-volume samples of a single biopsy of colorectal tumor, a gene expression profile was successfully obtained and a differentially expressed gene set related to colorectal carcinogenesis was detectable, as when using whole tissue samples. The feasibility of microarray-based study using fine-needle aspiration biopsy (FNAB) samples in some human tumors and endoscopically obtained tissues from precancerous lesions such as Barrett's esophagus was also reported (34,35). These results suggested that low-volume tissue samples such as endoscopic biopsy might give an accurate picture of gene expression in the whole tumor.

The histopathological features are not always homogeneous within a solid tumor. In CRC, the surface and invasive front of the tumor are sometimes histopathologically different. The influence of such morphological intra-tumor heterogeneity on gene expression profiles is not clear, although heterogeneity was detected in individual genes (36). Heterogeneity based on the superficial area of the tumor would have an unfavorable impact on molecular diagnosis when biopsy samples are used. In our study, the gene expression profiles of paired biopsies from the same tumors were identical in almost all tumors. At the protein level, IHC also showed a homogeneous staining

pattern in cancer cells at the superficial position in 5 out of 7 genes. The heterogeneity in some varied genes at the protein level did not affect the intra-tumor homogeneity of the profiles at the transcriptional level. This may be because the use of tens to thousands of genes in profiling compensated for the difference due to heterogeneity in some varied genes or because the data at the transcriptional level do not always parallel those at the protein level (37).

Concerning the intra-tumor heterogeneity of the profiles in other cancers, differences in gene expression between cancer cells in the periphery and those in the center of breast cancers were detected using microdissected samples (38). However, only in a few candidate genes was the difference in the expression levels more than two-fold. In breast cancer, the profile of FNAB was reported to resemble closely that of the corresponding source tumor (39). In a comparison between FNABs and core biopsies, the difference in profiles within the same tumor was not greater than that between other tumors (40). Also in soft tissue sarcomas, the intra-tumor heterogeneity of the profiles was smaller than the inter-tumor heterogeneity (41).

It is not clear how many biopsies are sufficient to represent the biological properties of a tumor with gene expression profiles. The first part of our study indicated that the profile of one biopsy could distinguish cancers from adenomas, beyond the intra-tumor heterogeneity. However, our next pursuit is the differential diagnosis of more delicate and important differences, such as the potential of metastasis and sensitivity to chemo- or radio-therapy. Any unfavorable variation based on the sampling skill and the experiment may be a drawback on the actual clinical application of this method. Multiple biopsies from a tumor may be required to balance the differences within a tumor. The number of biopsies for microarray analysis was studied using biopsies from rectal epithelia and two biopsies per person were recommended, based on the equality of the expression data within a person (42), though similar analyses using biopsies from colorectal tumors have not reported.

Sampling techniques are important. Every biopsy was sampled by a specialist in the colonoscopic unit and very reliable sampling was carried out in this study. Inaccurate sampling would give confusing results showing a wide gap of profiles even between biopsies from one tumor. We took care to avoid contamination of the normal epithelium or adenomatous component on the periphery of the cancer tissue and confirmed the histology with pathological diagnosis of simultaneously obtained biopsies and surgical samples.

Our results suggest that gene expression profiling using endoscopic biopsies can accurately describe the biological properties of colorectal cancer. Further studies of gene expression profiling using preoperative endoscopic biopsies may allow the development of new diagnostic systems for the selection of neoadjuvant therapy or the method most appropriate for tumor resection. Ultimately, it may lead to individualized therapy for colorectal cancer.

References

1. Yiu HY, Whittemore AS and Shibata A: Increasing colorectal cancer incidence rates in Japan. Int J Cancer 109: 777-781, 2004.
2. Dukes CE: The classification of cancer of the rectum. J Pathol Bacteriol 35: 323-332, 1932.
3. Astler VB and Coller FA: The prognostic significance of direct extension of carcinoma of the colon and rectum. Ann Surg 139: 846-852, 1954.
4. Sobin LH and Witedkind CH (eds): TNM Classification of Malignant Tumors (5th edition). Wiley-Liss, New York, 1997.
5. Golub TR, Slonim DK, Tamayo P, *et al*: Molecular classification of cancer: class discovery and class prediction by gene expression monitoring. Science 286: 531-537, 1999.
6. Ramaswamy S and Golub TR: DNA microarrays in clinical oncology. J Clin Oncol 20: 1932-1941, 2002.
7. Alon U, Barkai N, Notterman DA, *et al*: Broad patterns of gene expression revealed by clustering analysis of tumor and normal colon tissues probed by oligonucleotide arrays. Proc Natl Acad Sci USA 96: 6745-6750, 1999.
8. Notterman DA, Alon U, Sierk AJ, *et al*: Transcriptional gene expression profiles of colorectal adenoma, adenocarcinoma, and normal tissue examined by oligonucleotide arrays. Cancer Res 61: 3124-3130, 2001.
9. Kitahara O, Furukawa Y, Tanaka T, *et al*: Alterations of gene expression during colorectal carcinogenesis revealed by cDNA microarrays after laser-capture microdissection of tumor tissues and normal epithelia. Cancer Res 61: 3544-3549, 2001.
10. Takemasa I, Higuchi H, Yamamoto H, *et al*: Construction of preferential cDNA microarray specialized for human colorectal carcinoma: molecular sketch of colorectal cancer. Biochem Biophys Res Commun 285: 1244-1249, 2001.
11. Lin YM, Furukawa Y, Tsunoda T, *et al*: Molecular diagnosis of colorectal tumors by expression profiles of 50 genes expressed differentially in adenomas and carcinomas. Oncogene 21: 4120-4128, 2002.
12. Zou TT, Selaru FM, Xu Y, *et al*: Application of cDNA microarrays to generate a molecular taxonomy capable of distinguishing between colon cancer and normal colon. Oncogene 21: 4855-4862, 2002.
13. Ichikawa Y, Ishikawa T, Takahashi S, *et al*: Identification of genes regulating colorectal carcinogenesis by using the algorithm for diagnosing malignant state method. Biochem Biophys Res Commun 296: 497-506, 2002.
14. Birkenkamp-Demtroder K, Christensen LL, Olesen SH, *et al*: Gene expression in colorectal cancer. Cancer Res 62: 4352-4363, 2002.
15. Williams NS, Gaynor RB, Scoggin S, *et al*: Identification and validation of genes involved in the pathogenesis of colorectal cancer using cDNA microarrays and RNA interference. Clin Cancer Res 9: 931-946, 2003.
16. Komori T, Takemasa I, Higuchi H, *et al*: Identification of differentially expressed genes involved in colorectal carcinogenesis using a cDNA microarray. J Exp Clin Cancer Res 23: 521-527, 2004.
17. Wang Y, Jatkoe T, Zhang Y, *et al*: Gene expression profiles and molecular markers to predict recurrence of Dukes' B colon cancer. J Clin Oncol 22: 1564-1571, 2004.
18. Bertucci F, Salas S, Eysteries S, *et al*: Gene expression profiling of colon cancer by DNA microarrays and correlation with histoclinical parameters. Oncogene 23: 1377-1391, 2004.
19. Kwon HC, Kim SH, Roh MS, *et al*: Gene expression profiling in lymph node-positive and lymph node-negative colorectal cancer. Dis Colon Rectum 47: 141-152, 2004.
20. Li M, Lin YM, Hasegawa S, *et al*: Genes associated with liver metastasis of colon cancer, identified by genome-wide cDNA microarray. Int J Oncol 24: 305-312, 2004.
21. Arango D, Laiho P, Kokko A, *et al*: Gene-expression profiling predicts recurrence in Dukes' C colorectal cancer. Gastroenterology 129: 874-884, 2005.
22. Yamasaki M, Takemasa I, Komori T, *et al*: The gene expression profile represents the molecular nature of liver metastasis in colorectal cancer. Int J Oncol 30: 129-138, 2007.
23. Sauer R, Becker H, Hohenberger W, *et al*: Preoperative versus postoperative chemoradiotherapy for rectal cancer. N Engl J Med 351: 1731-1740, 2004.
24. Ghadimi BM, Grade M, Difilippantonio MJ, *et al*: Effectiveness of gene expression profiling for response prediction of rectal adenocarcinoma to preoperative chemoradiotherapy. J Clin Oncol 23: 1826-1838, 2005.
25. Watanabe T, Komuro Y, Kiyomatsu T, *et al*: Prediction of sensitivity of rectal cancer cells in response to preoperative radiotherapy by DNA microarray analysis of gene expression profiles. Cancer Res 66: 3370-3374, 2006.

26. Okabe S, Shia J, Nash G, *et al*: Lymph node metastasis in T1 adenocarcinoma of the colon and rectum. J Gastrointest Surg 8: 1032-1040, 2004.
27. Ito Y, Yoshida H, Matsuzuka F, *et al*: Expression of the components of the Cip/Kip family in malignant lymphoma of the thyroid. Pathobiology 71: 164-170, 2004.
28. Chang JW, Jeon HB, Lee JH, *et al*: Augmented expression of peroxiredoxin I in lung cancer. Biochem Biophys Res Commun 289: 507-512, 2001.
29. Campa MJ, Wang MZ, Howard B, *et al*: Protein expression profiling identifies macrophage migration inhibitory factor and cyclophilin a as potential molecular targets in non-small cell lung cancer. Cancer Res 63: 1652-1656, 2003.
30. Pan Y, Bi F, Liu N, *et al*: Expression of seven main Rho family members in gastric carcinoma. Biochem Biophys Res Commun 315: 686-691, 2004.
31. Saramaki O, Willi N, Bratt O, *et al*: Amplification of EIF3S3 gene is associated with advanced stage in prostate cancer. Am J Pathol 159: 2089-2094, 2001.
32. Hisamatsu T, Watanabe M, Ogata H, *et al*: Interferon-inducible gene family 1-8U expression in colitis-associated colon cancer and severely inflamed mucosa in ulcerative colitis. Cancer Res 59: 5927-5931, 1999.
33. Clarke PA, George ML, Easdale S, *et al*: Molecular pharmacology of cancer therapy in human colorectal cancer by gene expression profiling. Cancer Res 63: 6855-6863, 2003.
34. Centeno BA, Enkemann SA, Coppola D, *et al*: Classification of human tumors using gene expression profiles obtained after microarray analysis of fine-needle aspiration biopsy samples. Cancer 105: 101-109, 2005.
35. EL-Seraq HB, Nurqalieva Z, Souza RF, *et al*: Is genomic evaluation feasible in endoscopic studies of Barrett's esophagus? A pilot study. Gastrointest Endosc 64: 17-26, 2006.
36. Kaio E, Tanaka S, Kitadai Y, *et al*: Clinical significance of angiogenic factor expression at the deepest invasive site of advanced colorectal carcinoma. Oncology 64: 61-73, 2003.
37. Nishizaki S, Charboneau L, Young L, *et al*: Proteomic profiling of the NCI-60 cancer cell line using new high-density reverse-phase lysate microarrays. Proc Natl Acad Sci USA 100: 14229-14234, 2003.
38. Zhu G, Reynolds L, Crnogorac-Jurcevic T, *et al*: Combination of microdissection and microarray analysis to identify gene expression changes between differentially located tumour cells in breast cancer. Oncogene 22: 3742-3748, 2003.
39. Assersohn L, Gangi L, Zhao Y, *et al*: The feasibility of using fine needle aspiration from primary breast cancers for cDNA microarray analyses. Clin Cancer Res 8: 794-801, 2002.
40. Symmans WF, Ayers M, Clark EA, *et al*: Total RNA yield and microarray gene expression profiles from fine-needle aspiration biopsy and core-needle biopsy samples of breast carcinoma. Cancer 97: 2960-2971, 2003.
41. Francis P, Fernebro J, Eden P, *et al*: Intratumor versus intertumor heterogeneity in gene expression profiles of soft-tissue sarcomas. Gene Chromosome Cancer 43: 302-308, 2005.
42. Pellis L, Franssen-van Hal NL, Burema J, *et al*: The intraclass correlation coefficient applied for evaluation of data correction, labeling methods, and rectal biopsy sampling in DNA microarray experiments. Physiol Genomics 16: 99-106, 2003.

ANTICANCER RESEARCH *28*: 179-186 (2008)

Pretreatment with S-1, an Oral Derivative of 5-Fluorouracil, Enhances Gemcitabine Effects in Pancreatic Cancer Xenografts

SHIN NAKAHIRA[1,2], SHOJI NAKAMORI[1,3], MASANORI TSUJIE[1,3], SETSUO TAKEDA[1], KEISHI SUGIMOTO[2], YUJI TAKAHASHI[1], JIRO OKAMI[1], SHIGERU MARUBASHI[1], ATSUSHI MIYAMOTO[1], YUTAKA TAKEDA[1], HIROAKI NAGANO[1], KEIZO DONO[1], KOJI UMESHITA[1], MASATO SAKON[1] and MORITO MONDEN[1]

[1]*Department of Surgery and Clinical Oncology, Graduate School of Medicine, Osaka University, E2, 2-2 Yamadaoka, Suita, Osaka 565-0871;*
[2]*Department of Surgery, Kansai Rosai Hospital, 3-1-69, Inabaso, Amagasaki, Hyogo 660-8511;*
[3]*Department of Surgery, Osaka National Hospital, National Hospital Organization, 2-1-14 Hoenzaka, Chuo-ku, Osaka 540-0006, Japan*

Abstract. *Background: The systemic administration of gemcitabine (GEM) has been accepted as a standard treatment for patients with advanced pancreatic cancer. The major mediator of cellular uptake of GEM is the human equilibrative nucleoside transporter 1 (hENT1) whose expression is up-regulated by thymidylate synthase inhibitors, such as 5-fluorouracil (5-FU). S-1 is a novel oral derivative of the 5-FU prodrug tegafur combined with two modulators. Recent clinical trials have reported the promising effect of S-1 in pancreatic cancer. The purpose of this study was to evaluate the relationship between different schedules and the effects of GEM/S-1 combination therapy on pancreatic cancer xenograft models. Materials and Methods: Human pancreatic tumor xenografts were prepared by subcutaneous implantation of MiaPaCa-2 into nude mice. Expression of hENT1 was determined by quantitative RT-PCR. GEM cellular uptake was determined using [^{3}H] GEM. Results: Significant increases in hENT1 expression and GEM cellular uptake were observed after S-1 treatment. Six different treatment schedules (no treatment, single agent of GEM or S-1, combination treatment with GEM either before, simultaneously or following administration of S-1) were compared. Significant tumor growth inhibition was observed in the mice treated with S-1 followed by GEM compared to either untreated mice or the mice treated with the other schedules. Conclusion: Based on the effects of S-1 on the uptake of GEM, S-1 should be used before GEM treatment. The GEM/S-1 combination therapy in patients with pancreatic cancer may be promising and should be tested in clinical trials.*

Correspondence to: Shoji Nakamori, MD, Ph.D., Chief Surgeon of Department of Surgery, Cancer Center, Head of Molecular Medicine, Osaka National Hospital, National Hospital Organization, 2-1-14 Hoenzaka, Chuo-ku, Osaka 540-0006, Japan. Tel: +81669421331, Fax: +81669436467, e-mail: nakamori@ onh.go.jp

Key Words: S-1, 5-fluorouracil, gemcitabine, human equilibrative nucleotide transporter, schedule-dependent effect, combination chemotherapy, *in vivo*, pancreatic cancer.

Gemcitabine (2',2'-difluorodeoxycytidine (dFdC); Gemzar), accepted as a standard chemotherapeutic agent for patients with advanced pancreatic cancer, is a cell cycle-dependent deoxycytidine analogue of the antimetabolic class. It must first be transported into the cell and then be phosphorylated to its active triphosphate form. Incorporation of gemcitabine triphosphate into DNA is most likely the major mechanism through which gemcitabine exerts its cytotoxic actions (1).

Cells can synthesize nucleotides either through a *de novo* synthesis pathway or a salvage pathway. 5-Fluorouracil (5-FU), one of the thymidylate synthase (TS) inhibitors, is known to act as a *de novo* synthesis inhibitor (2). In the salvage pathway, nucleosides and nucleobases must first be transported across the cell membrane by nucleoside transporter proteins. In addition to nucleosides, nucleoside analogues are also taken up into the cell *via* these specific transporters (3). Gemcitabine is a substrate for five of the nucleoside transporters found in humans (4). These are human equilibrative nucleoside transporter 1 (hENT1), hENT2, human concentrative nucleoside transporter 1 (hCNT1), hCNT2 and hCNT3. The most active gemcitabine uptake is *via* hENT1 (4). It has been reported that 5-FU leads to an increase in cell surface hENT1 (5, 6). An increase in hENT1 can potentially augment the effect of gemcitabine because this agent enters the cell *via* hENT1. In fact, it has also been reported that pretreatment of pancreatic cancer cell lines *in vitro* and *in vivo* with 5-FU augmented the effects of single-agent gemcitabine

0250-7005/2008 $2.00+.40

treatment, whereas concurrent treatment or gemcitabine prior to 5-FU did not (7, 8). These results suggest that the effect of gemcitabine/5-FU combination therapy could be dependent on the selected treatment schedule.

S-1 (TS-1) is an oral fluorinated pyrimidine which contains tegafur (FT), 5-chloro-2,4-dihydroxypyridine (CDHP) and potassium oxonate (Oxo) in a molar ratio of FT:CDHP:Oxo of 1:0.4:1, based on the biochemical modulation of 5-FU (9, 10). FT, a prodrug of 5-FU, is gradually converted to 5-FU and is rapidly catabolized by dihydropyrimidine dehydrogenase (DPD) in the liver. CDHP is a competitive inhibitor of 5-FU catabolism, being about 180 times more potent than uracil in inhibiting DPD (11). When combined with 5-FU, this results in the prolonged maintenance of 5-FU concentrations, both in plasma and in tumors. In addition, it has been suggested that CDHP has the potential to enhance the antitumor activity of 5-FU against subcutaneous tumors in nude mice, using human pancreatic carcinoma cells with a high tumoral DPD activity (12). Oxo is a selective inhibitor of phosphoribosyl pyrophosphate transferase in normal gastrointestinal tissues, resulting in decreased drug incorporation into cellular RNA and, therefore, in the reduction of gastrointestinal toxicity (13). Recent Phase II clinical trials using S-1 as a single agent have shown promising results in various solid tumors, particularly gastric and colorectal cancers, with a response rate of 31.6 to 53.6% and 16.7 to 39.5%, respectively (14). In patients with metastatic pancreatic cancer, a Phase II clinical trial showed the safety and efficacy of S-1, with a response rate of 37.5% and a median survival time of 8.8 months (15).

The relatively mild toxicity profile of gemcitabine has allowed for the development of gemcitabine-based combination chemotherapy regimens (16, 17). The combination of gemcitabine and 5-FU has been shown to have a marked synergistic cytotoxic effect including against pancreatic carcinoma cells in an *in vitro* assay (18, 19). The administration of oral S-1 is more convenient and simulates the effect of continuous infusion of 5-FU. However, no randomized Phase III trial has yet established the survival benefits of a combination of gemcitabine and 5-FU compared to gemcitabine alone (16, 17). Recently, two clinical trials of gemcitabine and S-1 have demonstrated favorable response and tolerability with different dose and schedule (20, 21). Therefore, we focused on optimizing the efficacy of gemcitabine through modification of the schedule of these two agents.

The purpose of the present study was to evaluate the relationship between the schedules of gemcitabine/S-1 combination therapy and their effects in pancreatic cancer. We hypothesized that pretreatment with S-1 would increase hENT1 and thus increase the cytotoxicity of gemcitabine, which enters the cell *via* hENT1, in pancreatic cancer.

Materials and Methods

Cell culture. In a previous study, we selected three human pancreatic carcinoma cell lines which showed a higher rate of 5-FU-induced increase in hENT1 mRNA, however, we failed to establish subcutaneous tumors except for MiaPaCa-2, hence the human pancreatic carcinoma cell line MiaPaCa-2 was used in the present study (8). MiaPaCa-2 was obtained from the Japanese Collection of Research Bioresources (JCRB, Japan) and was cultured at 37°C under 5% CO_2 in Dulbecco's modified Eagle's medium (DMEM) (Sigma Chemical Co., St. Louis, MO, USA) supplemented with 10% fetal bovine serum (FBS) (Hyclone Laboratories, Inc., Rockville, MD, USA) and 100 units/ml each of penicillin and streptomycin.

Drugs and reagents. S-1 (TS-1) and gemcitabine (GEMZAR) were kindly provided by Taiho Pharmaceutical Co., Ltd (Tokyo, Japan) and Eli Lily, Japan (Indianapolis, IN, USA) respectively. [^{3}H] Gemcitabine was purchased from Moravek Biochemicals, Inc. (Brea, CA, USA). All drugs were dissolved in distilled water.

Pancreatic cancer xenograft model and treatment. The experimental protocol was approved by the Ethics Review Committee for Animal Experimentation of Graduate School of Medicine, Osaka University. Four-week-old female BALB/c *nu/nu* mice were purchased from Japan Clea (Tokyo, Japan) and maintained in specific pathogen-free conditions. Human pancreatic tumor xenografts were prepared by subcutaneous implantation of MiaPaCa-2 cells ($5x10^6$ cells/ 100 μl phosphate-buffered saline) into the right back of nude mice. When the tumors reached a volume between 100 and 200 mm^3, mice were randomly divided into treatment groups (n=5 for each group) according to tumor volume (day 0). S-1 was orally administrated at a dose of 10 mg/kg/day as described elsewhere (22), and gemcitabine was injected into the peritoneal cavity at a dose of 240 mg/kg as described elsewhere (23).

Quantitative reverse transcription-polymerase chain reaction (Q-RT-PCR). RNA extraction was carried out with TRIzol reagent (Invitrogen, Carlsbad, CA, USA) using a single-step method, and cDNA was generated with avian myeloblastosis virus reverse transcriptase (Promega, Madison, WI, USA), as described elsewhere (24). In this assay, porphobilinogen deaminase (PBGD) mRNA was used as an internal control (25). Q-RT-PCR was performed in a LightCycler apparatus using LightCycler Fast Start DNA Master SYBR Green I (Roche Diagnostics, Mannheim, Germany) according to the manufacturer's instructions. The PCR primers used for detection of PBGD and hENT1 cDNAs were synthesized as described elsewhere (25, 26). PCR was performed with cycling conditions of 95°C for 10 min, followed by 40 cycles of denaturation at 95°C for 10 s, annealing at 62°C for 10 s, and extension at 72°C for 20 s. To quantify the data, hENT1 mRNA levels were normalized by PBGD mRNA levels.

hENT1 mRNA expression and [^{3}H] gemcitabine uptake assay in vivo. The BALB/c mice bearing distinct MiaPaCa-2 tumors were divided into the following three groups of 6 mice each: (a) no treatment; (b) daily oral administration of S-1 for 5 consecutive days at a dose of 10 mg/kg/day (day 1 to 5); (c) daily oral administration of S-1 for 5 consecutive days at the dose of 50 mg/kg/day (days 1 to 5). On day 6, MiaPaCa-2 tumors in three of the mice killed by cervical dislocation of each group were removed and homogenized, and

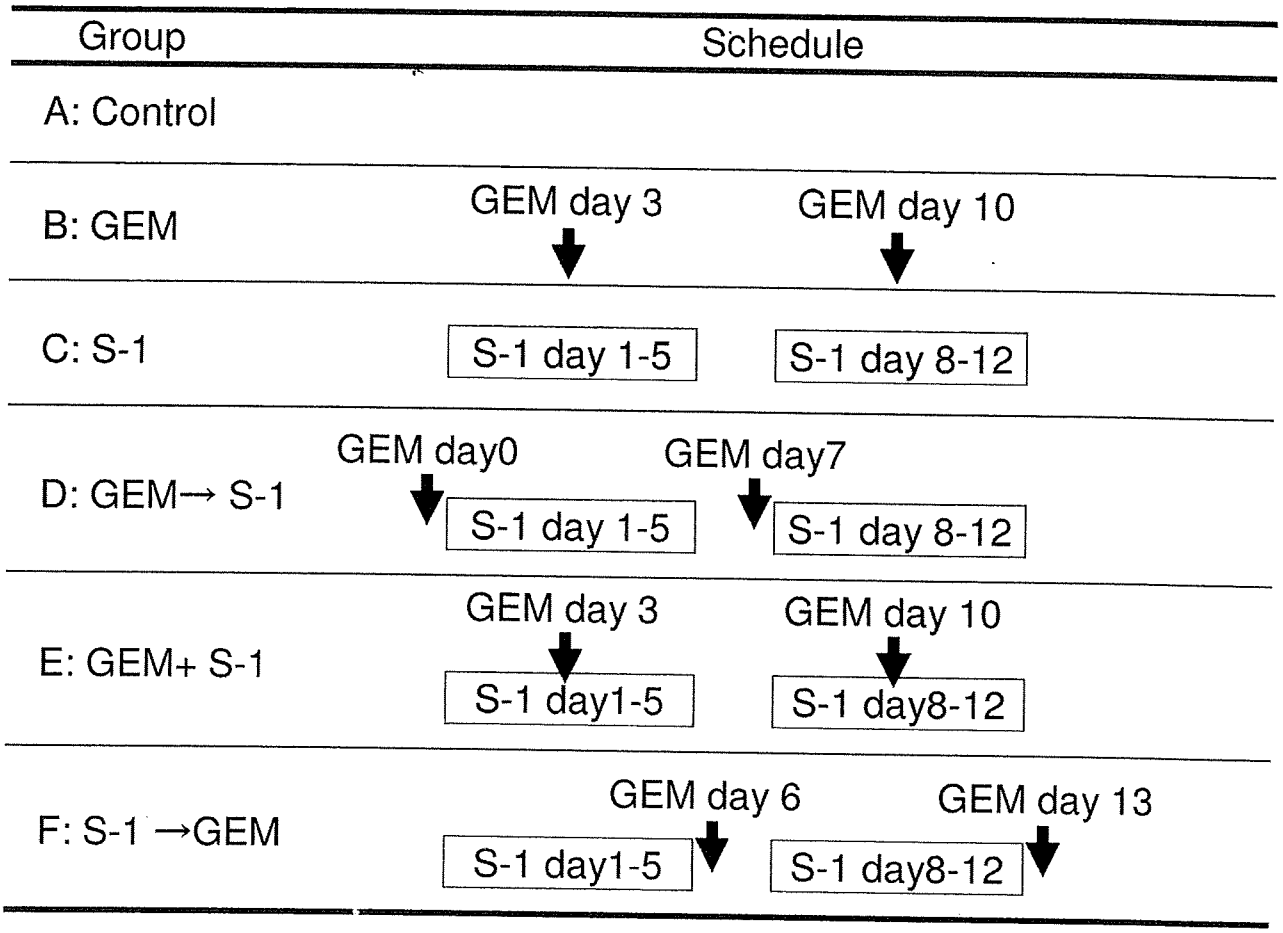

Figure 1. *Treatment schedule. MiaPaCa-2 cells ($5x10^6$ cells/100 μl phosphate-buffered saline) were injected subcutaneously into the right back of BALB/c mice. The mice were divided into 6 groups of 5 mice according to tumor volume. Gemcitabine (240 mg/kg) was administered by intraperitoneal injection and S-1 (10 mg/kg) by oral gavage. GEM: gemcitabine.*

quantitative gene expression of hENT1 mRNA in tumors was analyzed using LightCycler. The remaining three mice of each group were given a single intraperitoneal injection of [^{3}H] gemcitabine (240 mg/kg). Thirty minutes after gemcitabine injection, mice were killed by cervical dislocation, tumors were removed, weighed, and homogenized in Lumasolve solubilizer (LUMAC*LSC, Landgraaf, Netherlands). Gemcitabine concentrations in tumors were analyzed by quantitation of radioactivity as described elsewhere (27). The [^{3}H] gemcitabine uptakes were normalized by tumor weight.

Antitumor experiments in vivo. Mice bearing distinct tumors were randomly divided into the following six groups of 5 mice each (Figure 1): (A) no treatment; (B) weekly intraperitoneal injections of gemcitabine as a single agent (day 3, 10); (C) daily oral administrations of S-1 as a single agent for 5 consecutive days a week (day 1 to 5, day 8 to 12); (D) sequential combination treatment with gemcitabine (day 0, 7) prior to S-1 (day 1 to 5, day 8 to 12); (E) coadministrations of gemcitabine (day 3, 10) and S-1 (day 1 to 5, day 8 to 12); (F) sequential combination treatment with S-1 (day 1 to 5, day 8 to 12) prior to gemcitabine (day 6, 13). The animals were monitored for activity, physical condition, determination of body weight, and measurement of tumor volume [1/2 x (the major axis) x (the minor axis)^2] every other day. Statistical analysis of the data for the comparison of different groups was carried out using tumor volumes on day 18.

Statistical analysis. Statistical analysis was performed using the StatView J-5.0 program (Abacus Concepts, Inc., Berkeley, CA, USA). Data were expressed as the average of experiments and represented as mean±SD. Differences between groups were examined for statistical significance using ANOVA. In all analyses, values of $p<0.05$ were considered statistically significant.

Results

hENT1 mRNA expression in pancreatic cancer xenograft tumors. The effect of S-1 on the hENT1 mRNA expression in xenograft tumors of MiaPaCa-2 was examined using quantitative RT-PCR (Figure 2). After the daily oral administrations of S-1 for 5 consecutive days, the tumors in

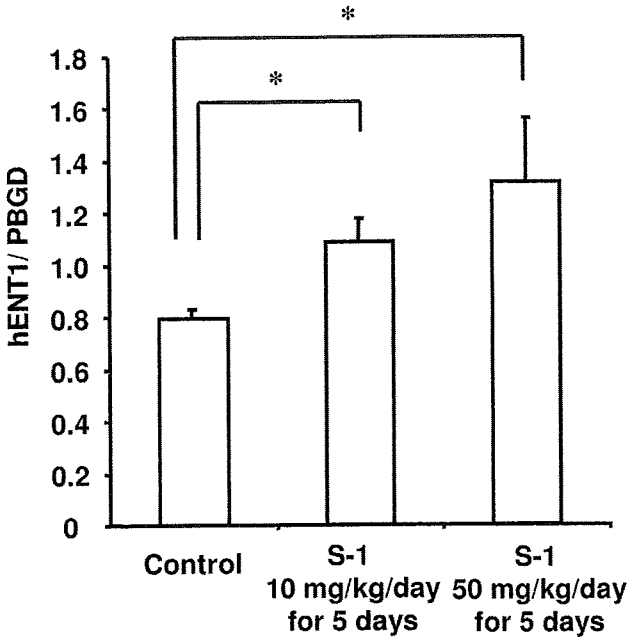

Figure 2. *Quantification of hENT1 mRNA expression in MiaPaCa-2 xenograft tumors treated with or without S-1. To quantify the data, hENT1 mRNA levels were normalized by PBGD mRNA levels. Results represent mean±SD (each group, n=3). The tumors in S-1 treated mice showed increased hENT1 levels. *p<0.05.*

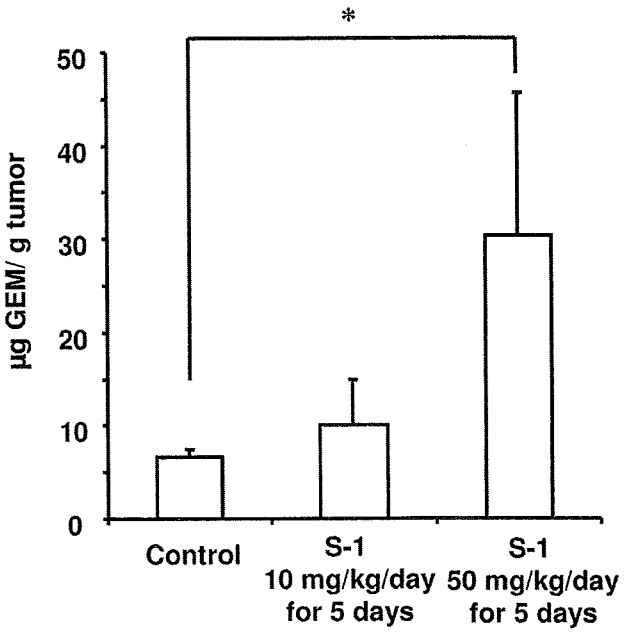

Figure 3. *Uptake of [^{3}H] gemcitabine after pretreatment with S-1 in pancreatic cancer xenograft tumors. The [^{3}H] gemcitabine uptakes were normalized by tumor weight. Results represent mean±SD (each group, n=3). The tumoral gemcitabine uptakes in S-1 treatment group at the dose of 50 mg/kg/day were significantly higher than the uptakes in control group. * p<0.05.*

S-1-treated mice showed increased hENT1 levels. The tumoral hENT1 expression in the S-1 treatment groups was significantly up-regulated compared with those in the control group.

Uptake of [^{3}H] gemcitabine after pretreatment with S-1 in pancreatic cancer xenograft tumors. The uptakes of gemcitabine were quantified using a [^{3}H] gemcitabine uptake assay (Figure 3). Although the S-1 treatment group at the dose of 10 mg/kg/day tended to show increased [^{3}H] gemcitabine uptake level, it was not significantly higher than that of the control group. However, the tumoral gemcitabine uptakes in S-1 treatment group at the dose of 50 mg/kg/day were significantly higher than the uptakes in the control group.

The schedule-dependent antitumor effect of gemcitabine and S-1 on human pancreatic tumor xenografts. The nude mice with the subcutaneous tumor were divided into six groups and treated as described in "Materials and Methods" and the antitumor effects were evaluated with the tumor volume at the day 18. The mean tumor volumes on day 18 were 4.2±1.5, 2.0±0.2, 2.3±1.0, 2.8±0.9, 2.1±0.7 and 1.0±0.3 cm^3 in Groups A, B, C, D, E and F, respectively (Figures 4 and 5). Tumor volumes of each treatment group were significantly smaller than those of the control group except for group D (GEM→S-1). Although there was not difference in tumor volumes among treatment groups B, C, D and E, statistically significant tumor growth inhibition was observed in Group F (S-1→GEM) compared with all the other treatment groups ($p<0.05$). Although the mice which were given S-1 first or simultaneously with gemcitabine showed stronger weight loss compared with other groups during and after the treatment, no mice died from the side-effects of the drugs or any other reasons up to the end of the study (day 18) (Figure 6).

Discussion

Although the systemic administration of gemcitabine is currently considered the standard first-line treatment for patients with advanced pancreatic cancer, single-agent gemcitabine has provided limited benefit, with objective response rates of less than 15% and a median survival of less than 6 months (28-30). Owing to the activity of gemcitabine, a variety of studies have now assessed its activity in combination with other agents. These studies have shown varying degrees of success, with no combination showing clear evidence of significantly superior activity (28). Combination of anticancer agents

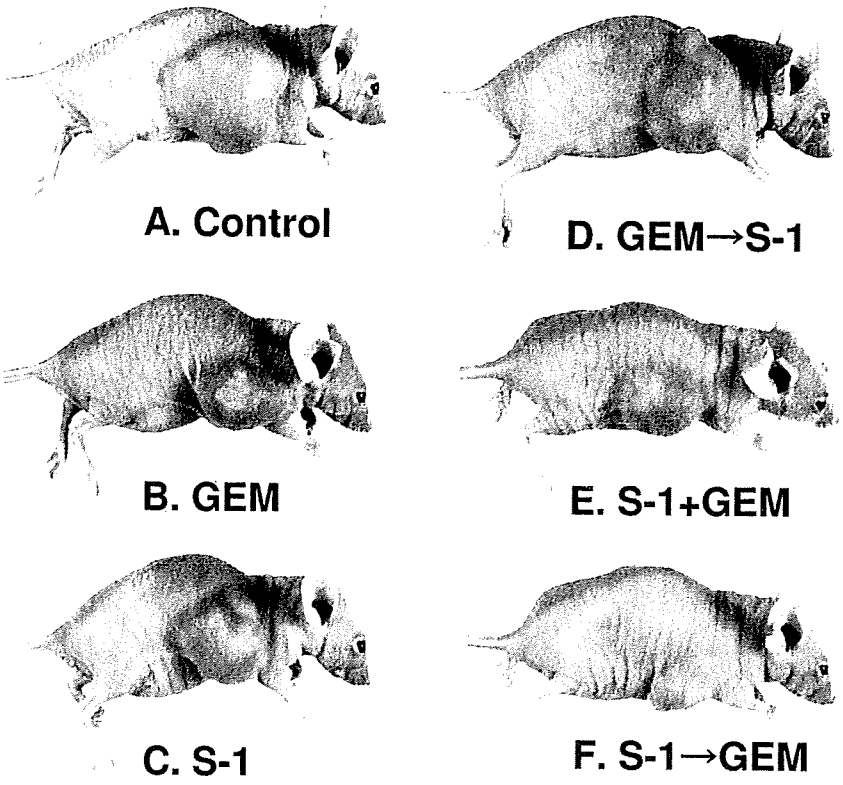

Figure 4. *BALB/c mice with subcutaneous human pancreatic tumor after treatment.*

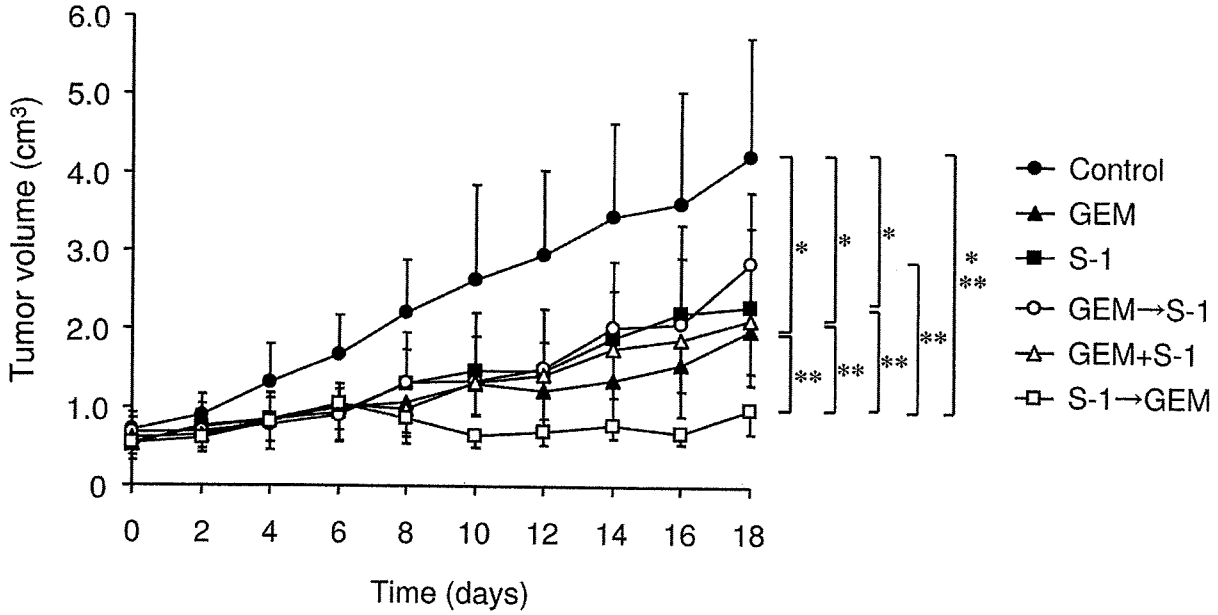

Figure 5. *Antitumor effect of the combination of gemcitabine with S-1 in vivo. Six different groups of the therapeutic experiments were carried out (Figure 1). Statistical analysis for the comparison of different groups was performed using tumor volumes on day 18. Results represent mean±SD (each group, n=5). Tumor volumes of each treatment group were significantly smaller than those of the control group except for group D (*p<0.05). Statistically significant growth inhibition was observed in Group F compared to all other treatment groups (**p<0.05). *,**p<0.05.*

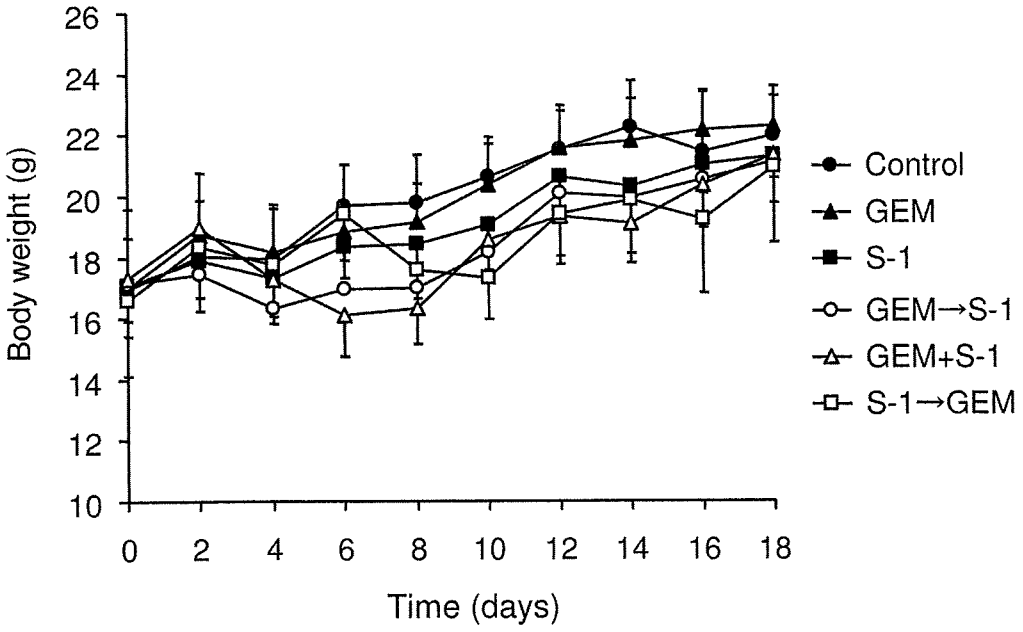

Figure 6. *Body weight curves of the mice. The corresponding tumor growth curves are shown in Figure 3. Results represent mean±SD (each group, n=5). There was no statistically significant difference between groups.*

has become a highly important modality for the treatment of cancer. Furthermore, combination chemotherapy is influenced by the employment of optimal scheduling (31). Gemcitabine is considered to be attractive for combination chemotherapy due to its mild toxicity profile at an active dose (16, 17).

However, in one study, the combination of 5-FU with gemcitabine did not improve the median survival of patients with advanced pancreatic carcinoma compared to single-agent gemcitabine (30). On the other hand, a novel oral derivative of 5-FU, S-1, was reported to have favorable results in pancreatic cancer patients (15), and a Phase II trial of S-1 combined with gemcitabine demonstrated promising efficacy with objective response rates of 48% and a median survival of 12.5 months (21). Therefore, we evaluated the effect of gemcitabine/S-1 combination therapy on human pancreatic cancer especially in terms of the schedule of the two drugs. Our study shows that the sequence can be an important factor in the antitumor activity of the combination of gemcitabine and S-1, and that hENT1 might play an important role in this effect.

The sequence-dependent effects of the combination of TS inhibitors and gemcitabine on human pancreatic cancer cells were reported to be seen with maximum effect when the TS inhibitors preceded gemcitabine *in vitro* (7). Moreover, this effect was not associated with basal hENT1 levels but with a significant increase in hENT1 levels caused by the TS inhibitors (7). Therefore, for *in vivo* experiments, we decided to use the cell lines which showed the highest rate of 5-FU induced increase in hENT1 mRNA (8).

We first examined the effects of S-1 on expression of hENT1 mRNA and gemcitabine cellular uptake in pancreatic cancer xenografts. 5-FU, known as a TS inhibitor, blocks the formation of 2'-deoxythymidine-5'-monophosphate (dTMP) and depletes intracellular nucleoside pools so that proliferating cells then depend on salvage of preformed nucleosides from extracellular fluid. 5-FU also up-regulates the amount of cell surface hENT1 as confirmed by flow cytometric analysis (7). In this study, we demonstrated that treatment with S-1 resulted in hENT1 up-regulation at the mRNA level and increased tumoral gemcitabine uptake.

To clarify the optimal schedule of treatment, we investigated the effect of six different schedules of treatment of S-1 and/or gemcitabine on a xenograft model of MiaPaCa-2 tumors. We did not detect any significant differences among the monotherapy groups and combination groups except for the S-1 followed by gemcitabine group. However, significant tumor growth inhibition was observed in mice treated with S-1 followed by gemcitabine compared with either untreated mice or the other treatment groups. Moreover, the synergistic tumor growth inhibitory effect was observed only in the S-1 followed by gemcitabine group and not in the other

combination groups. These results suggest that the schedule in which the gemcitabine is administered after S-1 could be the optimal combination of these two agents in the treatment of pancreatic cancer. The up-regulation of hENT1 induced by S-1 may play an important role in the enhanced growth inhibitory effect of gemcitabine.

Moreover, only the gemcitabine followed by S-1 treatment group did not show any efficacy compared with the control group. Previous reports showed that treatment of gemcitabine increased hENT1 expression and reduced 5-FU sensitivity in human pancreatic cancer cell lines (7). Therefore, the pretreatment with gemcitabine might reduce the effects of 5-FU due to the increasing supply of nucleosides and nucleobases *via* the salvage pathway. Indeed, the expression level of basal hENT1 was inversely associated with 5-FU sensitivity in human pancreatic cancer cell lines (8). These data suggested that the lack of benefit with sequences other than that of S-1 followed by gemcitabine *in vivo* might be due to gemcitabine-induced up-regulation of hENT1 and subsequent reduced 5-FU sensitivity.

It has been reported that mouse ENT1 (mENT1) mRNA was highly expressed in the heart, spleen, lung, liver and testes, and that lower levels of expression were detected in the brain and kidney (32). Therefore, enhanced gemcitabine effects induced by S-1 may also aggravate gemcitabine-induced side-effects. However, in this study, neither severe side-effects nor mortality were observed, although the mice treated with S-1 first or simultaneously with gemcitabine showed greater weight loss than other groups.

In conclusion, our results showed that the administration of S-1 followed by gemcitabine provides greater inhibitory effects than other gemcitabine/S-1 schedules in the treatment of pancreatic cancer.

Acknowledgements

This study was supported in part by Grants-in-Aid for Cancer Research from the Ministry of Health, Labour and Welfare, Japan; Scientific Research from the Japan Society for the Promotion of Science; Fund of Cancer Research from the Hyogo Prefecture Health Promotion Association; and a Grant-in-Aid for Community Health and Medical Care from the Ichou Association for Promotion of Medical Science.

References

1 Huang P, Chubb S, Hertel LW, Grindey GB and Plunkett W: Action of 2',2'-difluorodeoxycytidine on DNA synthesis. Cancer Res *51*: 6110-6117, 1991.

2 Thomas DM and Zalcberg JR: 5-Fluorouracil: a pharmacological paradigm in the use of cytotoxics. Clin Exp Pharmacol Physiol *25*: 887-895, 1998.

3 Baldwin SA, Mackey JR, Cass CE and Young JD: Nucleoside transporters: molecular biology and implications for therapeutic development. Mol Med Today *5*: 216-224, 1999.

4 Mackey JR, Mani RS, Selner M, Mowles D, Young JD, Belt JA, Crawford CR and Cass CE: Functional nucleoside transporters are required for gemcitabine influx and manifestation of toxicity in cancer cell lines. Cancer Res *58*: 4349-4357, 1998.

5 Pressacco J, Wiley JS, Jamieson GP, Erlichman C and Hedley DW: Modulation of the equilibrative nucleoside transporter by inhibitors of DNA synthesis. Br J Cancer *72*: 939-942, 1995.

6 Pressacco J, Mitrovski B, Erlichman C and Hedley DW: Effects of thymidylate synthase inhibition on thymidine kinase activity and nucleoside transporter expression. Cancer Res *55*: 1505-1508, 1995.

7 Rauchwerger DR, Firby PS, Hedley DW and Moore MJ: Equilibrative-sensitive nucleoside transporter and its role in gemcitabine sensitivity. Cancer Res *60*: 6075-6079, 2000.

8 Tsujie M, Nakamori S, Nakahira S, Takeda S, Takahashi Y, Hayashi N, Okami J, Nagano H, Dono K, Umeshita K, Sakon M and Monden M: Schedule-dependent therapeutic effects of gemcitabine combined with uracil-tegafur in a human pancreatic cancer xenograft model. Pancreas *33*: 142-147, 2006.

9 Shirasaka T, Nakano K, Takechi T, Satake H, Uchida J, Fujioka A, Saito H, Okabe H, Oyama K, Takeda S, Unemi N and Fukushima M: Antitumor activity of 1 M tegafur – 0.4 M 5-chloro-2,4-dihydroxypyridine – 1 M potassium oxonate (S-1) against human colon carcinoma orthotopically implanted into nude rats. Cancer Res *56*: 2602-2606, 1996.

10 Shirasaka T, Shimamato Y, Ohshimo H, Yamaguchi M, Kato T, Yonekura K and Fukushima M: Development of a novel form of an oral 5-fluorouracil derivative (S-1) directed to the potentiation of the tumor selective cytotoxicity of 5-fluorouracil by two biochemical modulators. Anticancer Drugs *7*: 548-557, 1996.

11 Tatsumi K, Fukushima M, Shirasaka T and Fujii S: Inhibitory effects of pyrimidine, barbituric acid and pyridine derivatives on 5-fluorouracil degradation in rat liver extracts. Jpn J Cancer Res *78*: 748-755, 1987.

12 Takechi T, Fujioka A, Matsushima E and Fukushima M: Enhancement of the antitumour activity of 5-fluorouracil (5-FU) by inhibiting dihydropyrimidine dehydrogenase activity (DPD) using 5-chloro-2,4-dihydroxypyridine (CDHP) in human tumour cells. Eur J Cancer *38*: 1271-1277, 2002.

13 Ogawa M: Novel anticancer drugs in Japan. J Cancer Res Clin Oncol *125*: 134-140, 1999.

14 Schoffski P: The modulated oral fluoropyrimidine prodrug S-1, and its use in gastrointestinal cancer and other solid tumors. Anticancer Drugs *15*: 85-106, 2004.

15 Furuse J, Okusaka T, Funakoshi A, Boku N, Yamao K, Ohkawa S and Saito H: A phase II study of S-1 in patients with metastatic pancreatic cancer (abstract 4104). Proc Am Soc Clin Oncol *23*: 333, 2005.

16 Kulke MH: Advanced pancreatic cancer: is there a role for combination therapy? Expert Rev Anticancer Ther *3*: 729-739, 2003.

17 El-Rayes BF and Philip PA: Systemic therapy for advanced pancreatic cancer. Expert Rev Anticancer Ther *2*: 426-436, 2002.

18 Bruckner H, Zhou G, Haenel P, Szrajer L, Greenspan E and Kurbacher C: *Ex vivo* ATP tumor testing of gemcitabine for combination chemotherapy and biochemical modulation (abstract 2116). Proc Am Assoc Cancer Res *39*: 310a, 1998.

19 Ren Q, Kao V and Grem JL: Cytotoxicity and DNA fragmentation associated with sequential gemcitabine and 5-fluoro-2'-deoxyuridine in HT-29 colon cancer cells. Clin Cancer Res *4*: 2811-2818, 1998.

20 Ueno H, Okusaka T, Ikeda M, Ishiguro Y, Morizane C, Matsubara J, Furuse J, Ishii H, Nagase M and Nakachi K: A phase I study of combination chemotherapy with gemcitabine and oral S-1 for advanced pancreatic cancer. Oncology *69*: 421-427, 2005.

21 Nakamura K, Yamaguchi T, Ishihara T, Sudo K, Kato H and Saisho H: Phase II trial of oral S-1 combined with gemcitabine in metastatic pancreatic cancer. Br J Cancer *94*: 1575-1579, 2006.

22 Fukushima M, Satake H, Uchida J, Shimamoto Y, Kato T, Takechi T, Okabe H, Fujioka A, Nakano K, Ohshimo H, Takeda S and Shirasaka T: Preclinical antitumor efficacy of S-1: a new oral formulation of 5-fluorouracil on human tumor xenografts. Int J Oncol *13*: 693-698, 1998.

23 Braakhuis BJ, Ruiz van Haperen VW, Boven E, Veerman G and Peters GJ: Schedule-dependent antitumor effect of gemcitabine in an *in vivo* model system. Semin Oncol *22*: 42-46, 1995.

24 Tsujie M, Nakamori S, Okami J, Hayashi N, Hiraoka N, Nagano H, Dono K, Umeshita K, Sakon M and Monden M: Thiazolidinediones inhibit growth of gastrointestinal, biliary, and pancreatic adenocarcinoma cells through activation of the peroxisome proliferator-activated receptor gamma/retinoid X receptor alpha pathway. Exp Cell Res *289*: 143-151, 2003.

25 Finke J, Fritzen R, Ternes P, Lange W and Dolken G: An improved strategy and a useful housekeeping gene for RNA analysis from formalin-fixed, paraffin-embedded tissues by PCR. Biotechniques *14*: 448-453, 1993.

26 Garcia-Manteiga J, Molina-Arcas M, Casado FJ, Mazo A and Pastor-Anglada M: Nucleoside transporter profiles in human pancreatic cancer cells: role of hCNT1 in 2',2'-difluorodeoxycytidine-induced cytotoxicity. Clin Cancer Res *9*: 5000-5008, 2003.

27 Wang H, Li M, Rinehart JJ and Zhang R: Pretreatment with dexamethasone increases antitumor activity of carboplatin and gemcitabine in mice bearing human cancer xenografts: *in vivo* activity, pharmacokinetics, and clinical implications for cancer chemotherapy. Clin Cancer Res *10*: 1633-1644, 2004.

28 Li D, Xie K, Wolff R and Abbruzzese JL: Pancreatic cancer. Lancet *363*: 1049-1057, 2004.

29 Burris HA, 3rd, Moore MJ, Andersen J, Green MR, Rothenberg ML, Modiano MR, Cripps MC, Portenoy RK, Storniolo AM, Tarassoff P, Nelson R, Dorr FA, Stephens CD and Von Hoff DD: Improvements in survival and clinical benefit with gemcitabine as first-line therapy for patients with advanced pancreas cancer: a randomized trial. J Clin Oncol *15*: 2403-2413, 1997.

30 Berlin JD, Catalano P, Thomas JP, Kugler JW, Haller DG and Benson AB, 3rd: Phase III study of gemcitabine in combination with fluorouracil *versus* gemcitabine alone in patients with advanced pancreatic carcinoma: Eastern Cooperative Oncology Group Trial E2297. J Clin Oncol *20*: 3270-3275, 2002.

31 Goldin A: Combined chemotherapy. Oncology *37(Suppl 1)*: 3-8, 1980.

32 Choi DS, Handa M, Young H, Gordon AS, Diamond I and Messing RO: Genomic organization and expression of the mouse equilibrative, nitrobenzylthioinosine-sensitive nucleoside transporter 1 (ENT1) gene. Biochem Biophys Res Commun *277*: 200-208, 2000.

Received June 15, 2007
Revised November 26, 2007
Accepted December 17, 2007

EUROPEAN JOURNAL OF CANCER 44 (2008) 885–897

available at www.sciencedirect.com

ScienceDirect

journal homepage: www.ejconline.com

Molecular mapping of human hepatocellular carcinoma provides deeper biological insight from genomic data

Nobuyoshi Kittaka[a], *Ichiro Takemasa*[a,*], *Yutaka Takeda*[a], *Shigeru Marubashi*[a], *Hiroaki Nagano*[a], *Koji Umeshita*[a], *Keizo Dono*[a], *Kenichi Matsubara*[b], *Nariaki Matsuura*[c], *Morito Monden*[a]

[a]*Department of Surgery, Graduate School of Medicine, Osaka University, 2-2 Yamadaoka E-2, Suita, Osaka 565-0871, Japan*
[b]*DNA Chip Research Inc., 1-1-43 Suehirocho, Tsurumi-ku, Yokohama 230-0045, Japan*
[c]*Department of Functional Diagnostic Science, Osaka University Graduate School of Medicine, 1-7 Yamadaoka, Suita, Osaka 565-0871, Japan*

ARTICLE INFO

Article history:
Received 5 December 2007
Received in revised form
5 February 2008
Accepted 12 February 2008
Available online 11 March 2008

Keywords:
DNA microarray
Network analysis
Integrative method
'Hotspot' region
Biological insight

ABSTRACT

DNA microarray analysis of human cancer has resulted in considerable accumulation of global gene profiles. However, extraction and understanding the underlying biology of cancer progression remains a significant challenge. This study applied a novel integrative computational and analytical approach to this challenge in human hepatocellular carcinoma (HCC) with the aim of identifying potential molecular markers or novel therapeutic targets. We analysed 100 HCC tissue samples by human 30 K DNA microarray. The gene expression data were uploaded into the network analysis tool, and the biological networks were displayed graphically. We identified several activated 'hotspot' regions harbouring a concentration of upregulated genes. Several 'hotspot' regions revealed integrin and Akt/NF-κB signalling. We identified key members linked to these signalling pathways including osteopontin (SPP1), glypican-3 (GPC3), annexin 2 (ANXA2), S100A10 and vimentin (VIM). Our integrative approach should significantly enhance the power of microarray data in identifying novel potential targets in human cancer.

1. Introduction

Investigation of various cancers at the molecular level is well underway through functional approaches including DNA microarray technology that can simultaneously detect the expression levels of tens of thousands of genes. The resulting wealth of data has been analysed with a variety of clustering, partitioning and pattern-matching algorithms in the quest to generate molecular signatures for several human malignant tumours with respect to their stage, prognostic outcome and response to therapy.

Notwithstanding the obvious power of the genomic data generated, these molecular analyses have not yielded the expected advances in our understanding of the mechanisms of cancer development, or the identification of critical genomic and molecular aberrations that would improve the precision of diagnosis or serve as therapeutic targets. This is mainly due to the overwhelming diversity of genome-wide interactions and gene-expression patterns, which limit effective learning from experimental data alone. Network analysis technologies are currently addressing this problem by mapping the gene expression data into relevant networks based on known mammalian biology, derived from basic and clinical research. To this end, our group has combined microarray analysis with a computational tool to obtain further biological insights into the regulatory networks of differentially expressed genes and

* *Corresponding author:* Tel.: +81 6 6879 3251; fax: +81 6 6879 3259.
E-mail address: alfa-t@sf6.so-net.ne.jp (I. Takemasa).
0959-8049/$ - see front matter © 2008 Elsevier Ltd. All rights reserved.
doi:10.1016/j.ejca.2008.02.019

the corresponding canonical pathways related to the progression of cancer. We applied this integrative approach to human hepatocellular carcinoma (HCC), the fifth most common malignancy worldwide.[1,2] Despite the remarkable improvements in diagnosis and patient management, the outcome for patients with HCC remains grave, mainly due to the advanced tumour stage accelerated by intrahepatic tumour spread and frequent tumour recurrence.[3] Hepatocarcinogenesis is a multistep process involving somatic mutations, loss of tumour suppressor genes and possibly the activation or overexpression of certain oncogenes.[4] These events lead to changes in the expression of numerous genes, and comparison of gene expression patterns between HCC and normal liver tissue is a popular method for characterising tumour properties and identifying novel target genes for possible therapy. However, this method has not proven to be sufficiently definitive in identifying genetic determinants of specific HCC regulatory pathways. New approaches are urgently needed to better understand the underlying mechanisms of hepatocarcinogenesis, and to develop new therapeutic approaches targeted to HCC-specific molecular abnormalities. By highlighting several activated regions in the genome (known as 'hotspot' regions[5,6]) involved in regulating the progression of HCC, we have identified significantly upregulated genes linked to these 'hotspot' pathways as potential key molecules.

Our integrative analysis revealed two 'hotspot' canonical pathways (integrin and Akt/NF-κB signalling pathways) and identified five potential key genes that were upregulated in the majority of HCC tumours. We further investigated two of these potential key molecules, ANXA2 and S100A10, which were upregulated at the protein and mRNA levels in most HCC samples. Importantly, because it is proteins that function in networks controlling critical cellular events,[7] it is reasonable to speculate that coexpression of ANXA2 and S100A10 at the protein level might have an impact on hepatocarcinogenesis through the activated 'hotspot' pathway.

2. Materials and methods

2.1. Tissue samples

Samples from 100 HCC tissues and seven normal livers without virus infection were obtained with informed consent from patients who underwent hepatic resection at Osaka University Hospital from 1997 to 2003. Tissue specimens (approximately 5 mm^3) for RNA isolation were stored at −80 °C until use. All tissue specimens were submitted for routine pathological evaluation and confirmation of diagnosis. The histopathological characterisation of HCC was based on the Classification of the Liver Cancer Study Group of Japan. Table 1 lists the clinicopathological features of the 100 cases of HCC.

2.2. Extraction and quality assessment of RNA

Total RNA was purified from tissue samples using TRIzol reagent (Invitrogen, San Diego, CA) as described by the manufacturer. The integrity of RNA was assessed on an Agilent 2100 Bioanalyzer and RNA 6000 LabChip kits (Yokokawa Ana-

Table 1 – Clinicopathological characteristics of 100 patients with HCC

Clinicopathological features	n
Age	
Median	66
Range	47–81
Gender	
Male	81
Female	19
Virus	
HBV	21
HCV	40
Both	28
None	11
Child-Turcotte-Pugh stage	
A	77
B	23
C	0
Liver cirrhosis	
Present	42
Absent	58
AFP	
<200 ng/ml	71
⩾200 ng/mg	29
PIVKA-II	
<50mAU/ml	36
⩾50mAU/ml	64
Tumour size	
<5.0 cm	76
⩾5.0 cm	24
Edmonson grading	
1–2	43
3–4	57
Histologic type of tumour	
Well differentiated	4
Moderately differentiated	41
Poorly differentiated	55
Vascular invasion	
Present	41
Absent	59
Intrahepatic metastasis	
Present	22
Absent	78
Pathological stage	
I	23
II	52
III	20
IVA	5
CLIP score	
0	56
1	35
2	8
3	0
4	1
5	0
6	0
JIS score	
0	18
1	46
2	26
3	9
4	1
5	0

CLIP score; The cancer of Liver Italian Program score.
JIS score; The Japan Integrated Staging score.

lytical Systems, Tokyo, Japan). Only high-quality RNA with intact 18s and 28s RNA was used for subsequent analysis. Seven RNA extractions from different normal liver tissue were mixed as the control reference.

2.3. *Preparation of fluorescently labelled aRNA targets and hybridisation*

Extracted RNA samples were amplified with T7 RNA polymerase using the Amino Allyl MessageAmp™ aRNA kit (Ambion, Austin, TM) according to the protocol provided by the manufacturer. The quality of each Amino Allyl-aRNA sample was checked on the Agilent 2100 Bioanalyzer. Five micrograms of control and experimental aRNA samples were labelled with Cy3 and Cy5, respectively, mixed and hybridised on an oligonucleotide microarray covering 30,336 human probes (AceGene Human 30K; DNA Chip Research Inc. and Hitachi Software Engineering Co., Yokohama, Japan). The experimental protocol is available at http://www.dna-chip.co.jp/thesis/AceGeneProtocol.pdf. The microarrays were scanned on a ScanArray 4000 (GSI Lumonics, Billerica, MA).

2.4. *Analysis of microarray data*

Signal values were calculated using DNASIS Array Software (Hitachi Software Inc., Tokyo). Following background subtraction, data with low signal intensities were excluded from additional investigation. In each sample, the Cy5/Cy3 ratio values were log-transformed. Then, global equalisation to remove a deviation of the signal intensity between whole Cy3- and Cy5-fluorescence was performed by subtracting the median of all log(Cy5/Cy3) values from each log(Cy5/Cy3) value. Genes with missing values in more than 20% of samples were excluded from further analysis; a total of 16,923 genes out of 30,336 were available for analysis.

2.5. *Gene network analysis*

We further analysed the signature genes of HCC by Ingenuity Pathways Analysis (Ingenuity systems, Mountain View, CA; http://www.ingenuity.com), a web-delivered application that enables biologists to discover, visualise and explore relevant networks significant to their experimental results, such as gene expression array datasets. The application makes use of the Ingenuity Pathways Knowledge Base (IPKB), which contains large amounts of individually modelled relationships between gene objects (e.g., genes, mRNAs and proteins) to dynamically generate significant biological networks and pathways. The submitted genes that are mapped to the corresponding gene objects in the IPKB are called 'focus genes'. The focus genes are used as the starting point for generating biological networks. To start building a network, the Ingenuity software queries the IPKB for interactions between focus genes and all the other genes stored in the IPKB, and then generates a set of networks with a maximum network size of 35 genes. A p value for each network is calculated according to the fit of the user's set of significant genes. This is accomplished by comparing the number of focus genes that participate in a given network relative to the total number of occurrences of those genes in all networks stored in the IPKB. The score of a network is displayed as the negative log of the p value, indicating the probability that a collection of genes equal to or greater than the number in a network could be achieved by chance alone.

2.6. *Selection of candidate genes expressed in HCC*

To identify molecular pathways that may be activated or suppressed in HCC, we used a network knowledge-base approach, Ingenuity Pathway Analysis Software, to analyse genome-wide transcriptional responses in the context of known functional interrelationships amongst proteins, small molecules and phenotypes. The post-normalised genes (16,923 genes) either up- or down-regulated in the microarray data, were uploaded into the IPKB as a tab-delimited text file of GenBank accession numbers. These biological networks comprising 5936 genes are displayed graphically as nodes (genes/gene products) and edges (the biological relationships between the nodes). The nodes are displayed using various shapes that represent the functional class of the gene product. The colour green reflects downregulation of gene expression, and red represents upregulation of gene expression with the significance of that regulation represented by colour intensity. Edges are displayed with various labels that describe the nature of the relationship between the nodes. In this way, simultaneous survey and evaluation of the subnetwork regions enabled us to identify several activated canonical pathways in HCC. We highlighted new molecules linked to the 'hotspot' canonical pathways.

2.7. *Real-time quantitative RT-PCR analysis*

Total RNA (1 μg) was used for reverse transcription, and complementary DNA (cDNA) was generated using the Reverse Transcription System (Promega, Madison, WI) as described previously.[8] Quantification of mRNA expression of the candidate genes listed in Table 2 was performed using a real-time thermal cycler, the LightCycler and detection system (Roche Diagnostics, Mannheim, Germany). For detection of the amplification products, LightCycler-DNA master SYBR green I (Boehringer

Table 2 – Candidate genes and expression ratio of microarray analysis

CDS ID	Gene symbol	Description	Average of Cy5/Cy3
NM_000582	SPP1	Secreted phosphoprotein 1 (osteopontin)	4.69
NM_004484	GPC3	Glypican 3	4.23
NM_004039	ANXA2	Annexin 2	2.86
M38591	S100A10	Cellular ligand of annexin 2	1.97
NM_003380	VIM	Vimentin	1.82

Mannheim, Mannheim, Germany) was used as described previously.[9] Briefly, a 20 μl reaction volume containing 2 μl of cDNA and 0.2 μmol/l of each primer was applied to a glass capillary. The primer sequences, PCR cycle conditions and annealing temperatures are listed in Supplementary Table 1. Quantitative analysis of mRNA was performed using LightCycler analysis software (Roche Diagnostics). The relative expression level of the candidate gene was computed with respect to the internal standard GAPDH mRNA to normalise for variations in the amount of input cDNA. The level of expression of the candidate gene was provided by the ratio, in which each normalised gene value in tissue samples was divided by GAPDH mRNA in the same control reference used in the microarray assay. We compared the ratio of candidate genes between samples randomly selected out of 100 HCC samples.

2.8. *Immunohistochemical staining*

Formalin-fixed, paraffin-embedded samples were cut into 5 μm sections, and these were deparaffinised in xylene and rehydrated through a graded series of ethanol. Immunohistochemical staining was performed using a Vectastain ABC peroxidase kit (Vector Labs, Burlingame, CA) as described previously.[10] Briefly, the sections were treated for antigen retrieval in 0.01 M sodium citrate buffer (pH 6.0) for 40 min at 95 °C, followed by incubation in methanol containing 0.3% hydrogen peroxide at room temperature for 20 min to block endogenous peroxidase. After blocking endogenous biotin, the sections were incubated with normal protein-block serum solution at room temperature for 20 min, to block non-specific staining, and then incubated overnight at 4 °C with anti-ANXA2 (mouse monoclonal IgG, diluted 1:500, Abcam Inc.), anti-S100A10 (mouse monoclonal IgG, diluted 1:400, Swant Inc.) and anti-GPC3 (mouse monoclonal IgG, University of Toronto, Jorge Filmus et al.[11]) as primary antibodies. After washing three times for 5 min in phosphate buffered saline (PBS), sections were incubated with a biotin-conjugated secondary antibody (horse anti-mouse for ANXA2, S100A10 and GPC3) at room temperature for 20 min and finally incubated with peroxidase-conjugated streptavidin at room temperature for 20 min. The peroxidase reaction was then developed with 3,3′-diaminobenzidine tetrachloride (Wako Pure Chemical Industries, Osaka, Japan). Finally, the sections were counterstained with Mayer's haematoxylin. For negative controls, sections were treated the same way except they were incubated with non-immunised rabbit IgG or Tris-buffered saline instead of the primary antibody. Immunohistochemical staining was assessed by two investigators independently, without the knowledge of the corresponding clinicopathological data.

2.9. *Statistical analysis*

Pearson's correlation coefficient, χ^2 test, t-test and Kaplan–Meier plot were analysed using StatView (Version 5.0) software (Abacus Concepts, Berkeley, CA). p values less than 0.05 were considered statistically significant. Hierarchical cluster analysis (HCA) was performed with Euclidean distance coefficient as a similarity coefficient and the unweighted pair group method using arithmetic averages (UPGMA) as the clustering algorithm, using GeneMaths (Version 2.0) software.

3. Results

3.1. *Microarray analysis of gene expression changes in HCC tumours*

Gene expression profiling of primary HCC tumours from 100 patients was examined by DNA microarray. We calculated the mean expression levels of each gene across all HCC samples, and, as a preliminary analysis, identified the top 2% of candidate genes displaying at least a 1.5-fold increase in expression. These highly upregulated genes included α-fetoprotein (AFP; data not shown), a common prognostic marker for HCC (fold change = 1.56), and GPC3, recently identified as a novel tumour marker of HCC (fold change = 4.23; fourth highest upregulation).

3.2. *Identification of biologically relevant networks and potential key genes highly expressed in HCC tumours*

In our global network comprising 5936 genes (Supplementary Fig. 1), we highlighted integrin and Akt/NF-κB signalling as two 'hotspot' pathways that comprised a concentration of upregulated genes. The integrin signalling pathway shown in Fig. 1A (gene subnetworks listed in Supplementary Table 2) was identified as significantly activated in HCC and contained 11 upregulated genes, flagging this pathway as a key regulator in HCC tumourigenesis. This fits with the role of integrin signalling in promoting cell proliferation and cell motility.[12] Furthermore, SPP1 and GPC3 were identified as potential key genes (upregulated with >1.5-fold change), with links to integrin signalling. Similarly, we identified the activation of the Akt/NF-κB pathway shown in Fig. 1B in HCC tumours (gene subnetworks listed in Supplementary Table 3). This signalling pathway contained 12 upregulated genes and plays key roles in many cell processes relevant to tumourigenesis including cell survival and apoptosis.[13] Amongst the genes linked to Akt/NF-κB signalling and that had >1.5-fold change were ANXA2, S100A10 and VIM. Network analysis revealed a link between Akt/NF-κB signalling and both ANXA2 and S100A10 through interactions with β-actin (ACTB) and E-cadherin (CDH1). These candidate genes are listed in Table 2.

3.3. *Quantitative RT-PCR validation of several selected genes*

To validate the microarray data, we performed quantitative RT-PCR for candidate genes in 20 samples randomly selected out of the 100 HCC tissues. We compared gene expression levels generated from quantitative RT-PCR with those from microarray analysis by Pearson's correlation coefficients for each candidate gene and StatView Software (Fig. 2). Each of the five genes analysed showed significant correlation confirming the results obtained by DNA microarray.

3.4. *Immunohistochemical study of glypican 3, Annexin 2 and S100A10 in patient samples*

Of the five genes overexpressed in HCC tumours by RT-PCR, immunohistochemical staining for GPC3 was performed on 10 samples of HCC and surrounding non-cancerous tissues

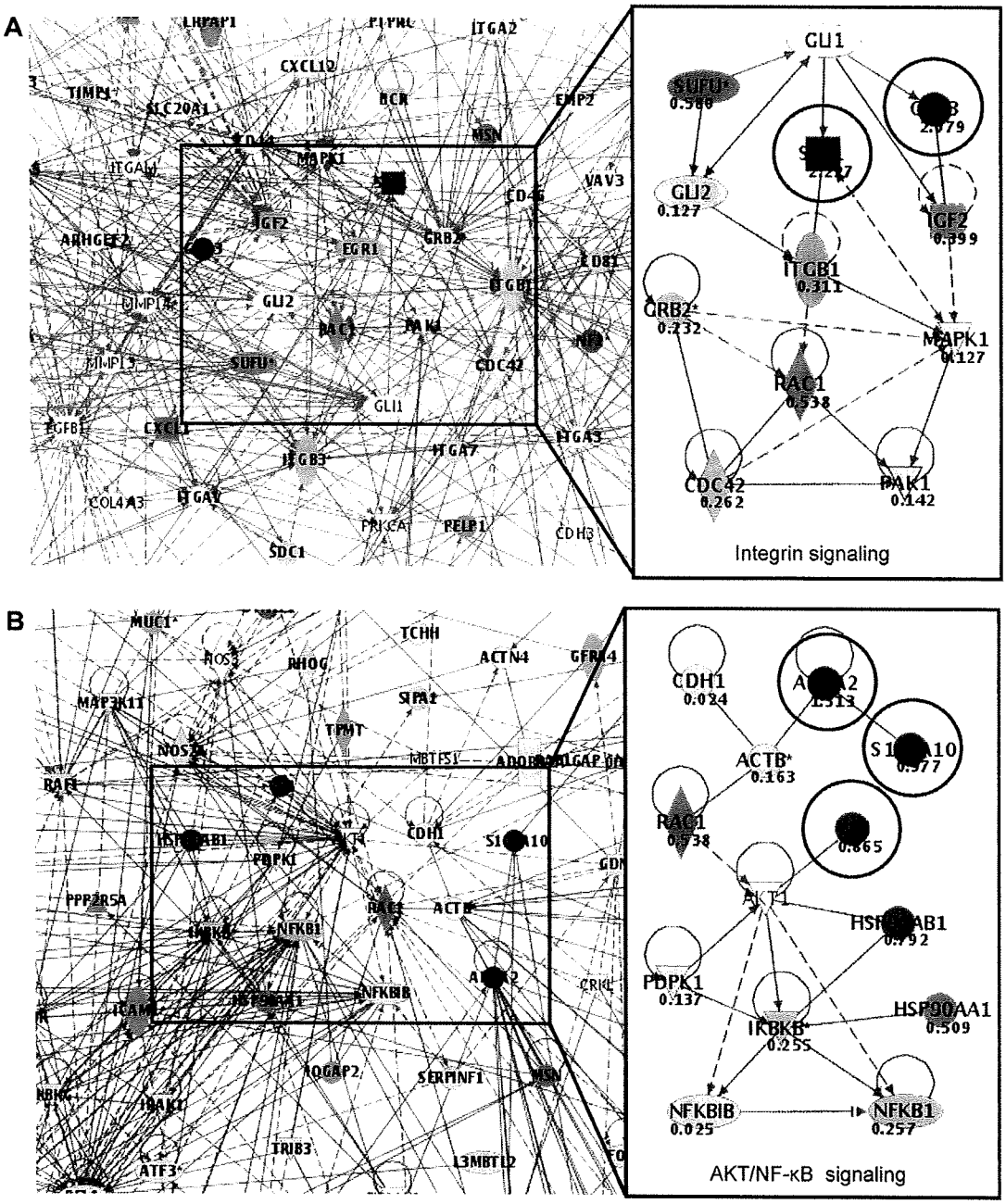

Fig. 1 – (A) The integrated method of DNA microarray and Ingenuity Pathway Analysis produced a network with 'hotspot' regions harbouring concentrations of upregulated genes. These genes included ITGB1 (integrin, beta 1), RAC1 (ras-related C3 botulinum toxin substrate 1), GRB2 (growth factor receptor-bound protein 2), CDC42 (cell division cycle 42), PAK1 (p21/Cdc42/Rac1-activated kinase 1) and MAPK1, which are all associated with integrin signalling. SPP1, GPC3, GLI1, GLI2, SUFU (suppressor of fused homolog) and IGF2 are also linked to this pathway. The circled genes, SPP1 and GPC3, were selected as candidate genes. The numerical value of each gene represents the median of all log(Cy5/Cy3) values. (B) The integrative method showed a second network including a 'hotspot' region. This region contained AKT1 (v-akt murine thymoma viral oncogene homolog 1), PDPK1 (3-phosphoinositide-dependent protein kinase-1), NFKBIB (nuclear factor of kappa light polypeptide gene enhancer in B-cells inhibitor, beta), NFKB1 (nuclear factor of kappa light polypeptide gene enhancer in B-cells 1), IKBKB (inhibitor of kappa light polypeptide gene enhancer in B-cells, kinase beta), HSP90AA1 (heat shock protein 90 kDa alpha, class A member 1) and HSP90AB1 (heat shock protein 90 kDa alpha, class B member 1), which are all associated with the Akt/NF-κB signalling pathway. ANXA2, S100A10, ACTB, CDH1 and VIM are also linked to this pathway. The circled genes, ANXA2, S100A10 and VIM, were selected as candidate genes. The numerical value of each gene represents the average of all log(Cy5/Cy3) values.

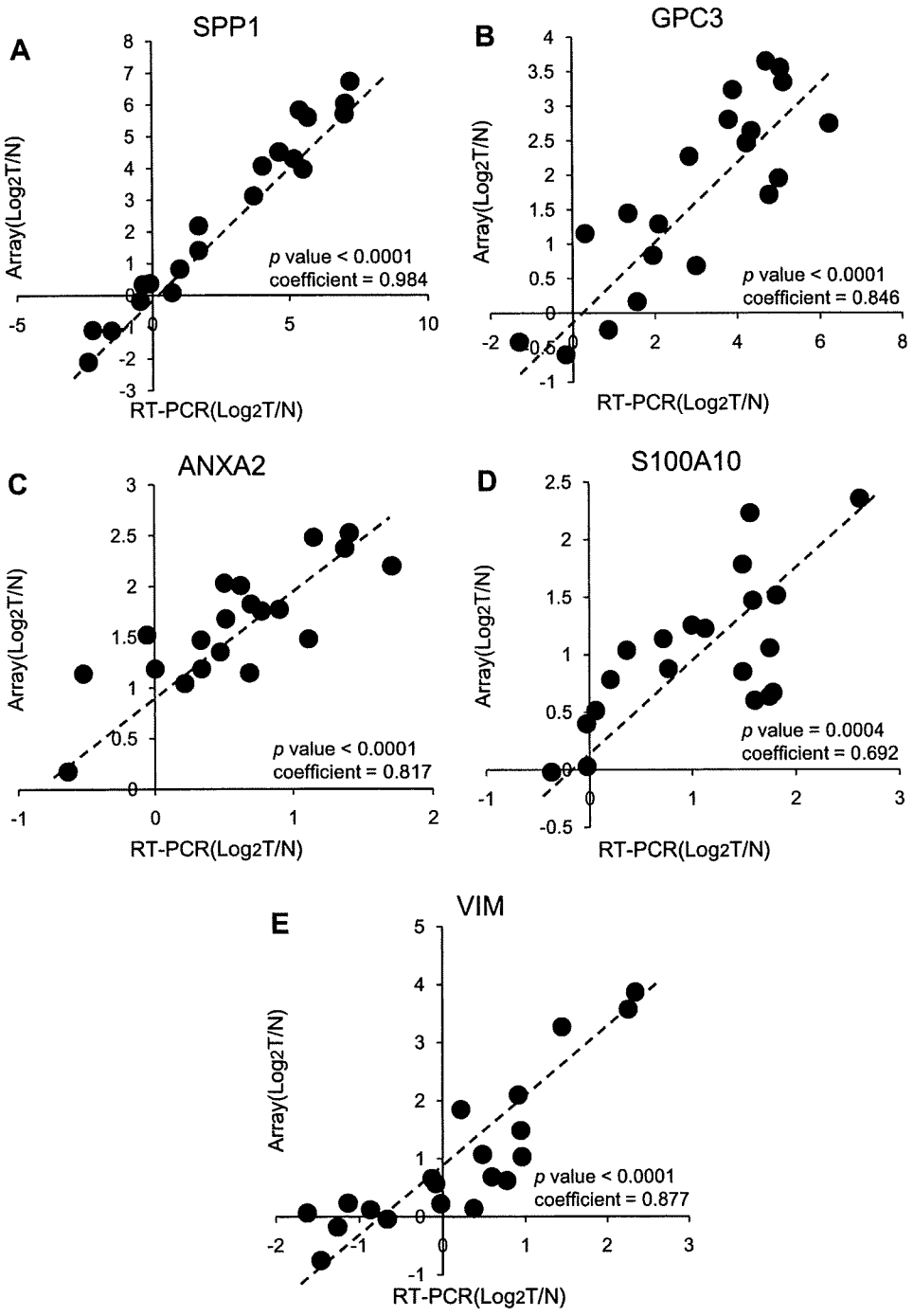

Fig. 2 – Results of quantitative RT-PCR on 20 samples randomly selected from the 100 HCC samples. Individual mRNA levels were normalised to GAPDH and expressed relative to those in a mixture of seven normal livers for SPP1, GPC3, ANXA2, S100A10 and VIM. We compared gene expression levels generated from quantitative RT-PCR with those from microarray analysis and used Pearson's correlation analysis for each candidate gene using StatView Software. (A), (B), (C), (D) and (E) show the correlation of SPP1, GPC3, ANXA2, S100A10 and VIM, respectively.

(Fig. 3A and B). GPC3 expression was observed in 7 of 10 cases of moderately or poorly differentiated HCC. As published previously,[11] staining of GPC3 was observed in a coarsely granular pattern near the cell membrane (2/7) and dispersed evenly in the cytoplasm (5/7). GPC3 expression was undetectable in all non-neoplastic tissues with diffuse hepatitis changes.

Immunohistochemical staining of ANXA2 and S100A10 was then performed on 20 paraffin-embedded samples of HCC and surrounding non-cancerous tissues. The Ca^{2+}-

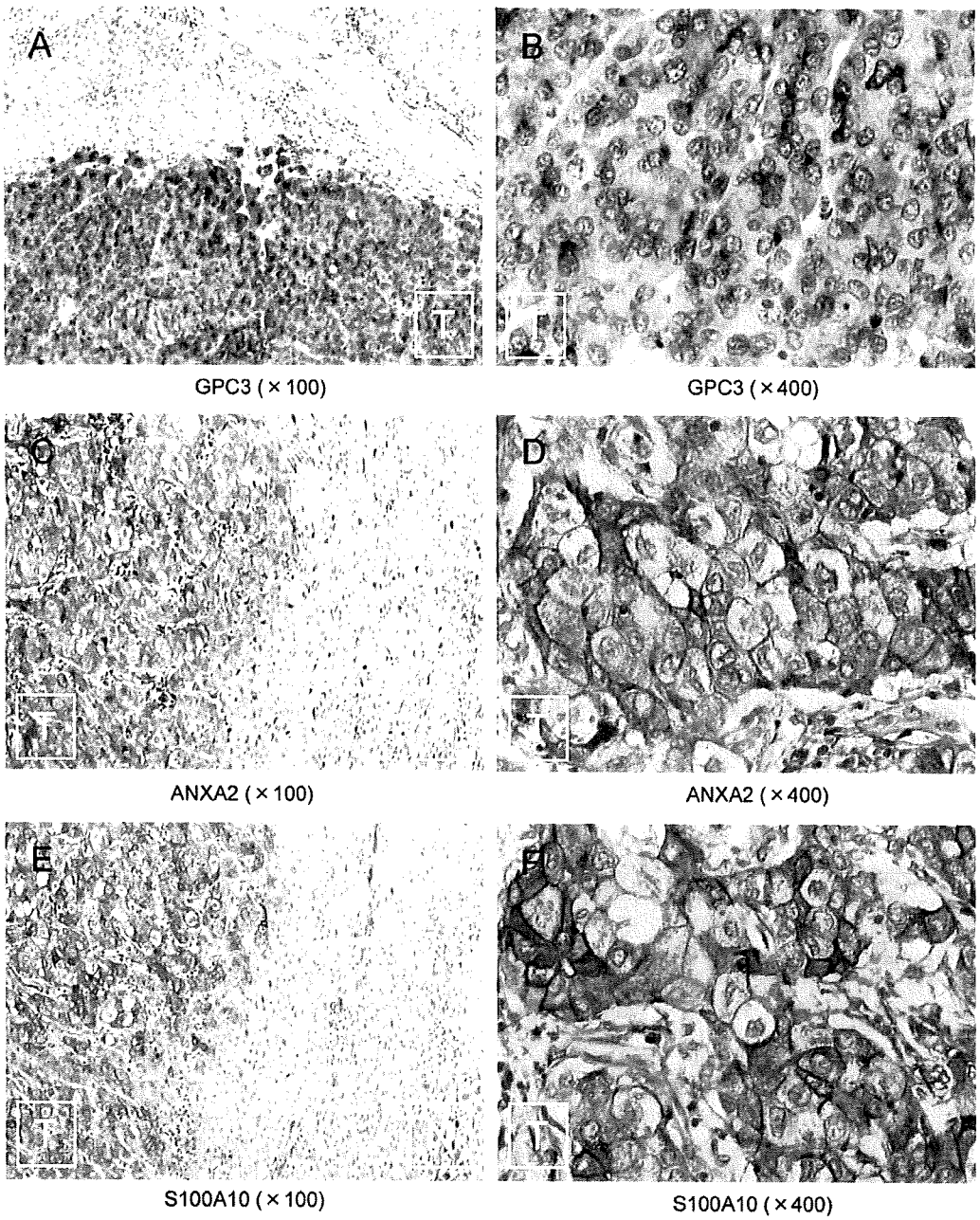

Fig. 3 – (A and B) GPC3 protein expression in human HCC tissue. Brown GPC3 immunostaining is evident in cancer cells. Note the diffuse non-granular staining pattern in the cytoplasm. (C and D) ANXA2 protein expression in human HCC tissue. Note ANXA2 staining in the cell membrane of cancer cells, with slight immunoreactivity in the cytoplasm. (E and F) S100A10 protein expression in human HCC tissues. Note S100A10 staining at the cell membrane of cancer cells. C, D, E and F are from the same tissue sample, and staining for S100A10 overlapped significant with ANXA2 staining. (A, C and E) ×100 magnification. (B, D and F) ×400 magnification. T; tumour region. N; normal liver.

and membrane-binding protein ANXA2 can form a hetero-tetrameric complex with S100A10 and this complex is thought to serve as a bridging or scaffolding function in the membrane underlying cytoskeleton.[14] Previous studies demonstrated both ANXA2 and S100A10 at the plasma membrane in hepatoblastoma HepG2 cell lines,[15] but not in human HCC tissues. Immunohistochemical staining of ANXA2 and S100A10 was stronger at the plasma membrane of the same samples than in the cytoplasm (Fig. 3C–F). The immunoreactivity for ANXA2 was heterogeneous, and cancerous tissues were immunopositive in 16 samples. Endothelial cells were immunopositive for ANXA2 in all samples tested. Similarly, staining of S100A10 was heterogeneous, and cancerous tissues were immunopositive in 17 samples.